Int. J. Multiphase Flow Vol. 6, pp. 281–294
Pergamon/Elsevier. 1980. Printed in Great Britain

THE EFFECT OF VIRTUAL MASS ON THE NUMERICAL STABILITY OF ACCELERATING TWO-PHASE FLOWS

R. T. LAHEY, JR, L. Y. CHENG, D. A. DREW and J. E. FLAHERTY
Rensselaer Polytechnic Institute, Troy, NY 12181, U.S.A.

(*Received* 7 *February* 1979; *in revised form* 8 *January* 1980)

Abstract—The effect of the virtual mass in accelerating two-phase flow was studied for various nozzle/diffuser flows. It was found that the final results were insensitive to virtual mass effects, but the numerical stability and efficiency was greatly improved. An analysis of the eigenvalues of the mathematical systems shows that virtual mass models improve numerical stability and efficiency by changing the nature of the eigenvalues.

INTRODUCTION

The ability to accurately and efficiently evaluate transient two-phase flow phenomena is needed to understand many processes of practical concern. For instance, nuclear reactor safety studies and the pressure-relief capabilities of many chemical reactors, require this ability.

Previous studies have indicated that numerical instabilities are frequently encountered when two-fluid models are numerically evaluated. These numerical problems have been shown (Bouré 1975) to be related to the modelling of the phasic interaction terms, and the resultant complex nature of the mathematical characteristics (Ramshaw & Trapp 1978).

Two distinct approaches are currently being taken to address this problem. One approach is to introduce so-called "numerical viscosity" into the numerical algorithm, to damp out high frequency instabilities which may occur due to imprecise modelling. This approach is an outgrowth of the single-phase gas dynamic techniques originally developed at the Courant Institute of NYU. It is currently being used in TRAC and other two-fluid digital computer codes being developed at LASL (Amsden & Harlow 1978). While this approach allows one to efficiently compute, the physical model veing evaluated is not generally alid, and thus inaccurate evaluations may result for some cases of practical concern.

The other, and most technically satisfying approach, is to accurately model the phasic interaction terms in the two-fluid model. These models consist of phasic mass, momentum and energy transfer laws. Of these interaction terms, the most important, from the point of view of numerical stability, are the momentum transfer terms, since they basically determine the characteristics of the mathematical system under consideration.

The most important momentum transfer laws are known (Ishii 1975) to be due to mass transfer effects, interfacial drag and virtual mass effects. The study presented in this paper was directed toward understanding the effect of virtual mass on the numerically stability of accelerating two-phase flows.

DISCUSSION

In order to simplify, and focus, this study, the special case of adiabatic air/water bubbly flow, through nozzles and diffusers, was considered. For this case, there is no mass transfer and thus all we need model are the interfacial drag (F_d) and the virtual mass (F_{vm}) forces. The latter force (F_{vm}) being due to the acceleration of the vapor bubbles relative to the liquid phase.

DETAILED NUMERICAL ANALYSIS

Following previous investigators (Wallis *et al.* 1976), one can assume a string of non-interacting bubbles flowing through a nozzle or diffuser. This assumption allows us to drop the temporal terms, since each bubble in the string will have the same velocity when it reaches a particular axial

location. The appropriate, one-dimensional momentum equations for the accelerating liquid and vapor bubble are, respectively,

$$(1-\alpha)\rho_L u_L \frac{du_L}{dz} = -(1-\alpha)\frac{dp}{dz} - (1-\alpha)\rho_L g\cos\phi + M_L - F_w, \quad [1]$$

$$\alpha\rho_G u_G \frac{du_G}{dz} = -\alpha\frac{dp}{dz} - \alpha\rho_G g\cos\phi + M_G, \quad [2]$$

where α is the volumetric vapor fraction; ρ_k is the density of phase-k; u_k is the axial phase velocity; p is the pressure; ϕ is the angle between the flow direction and the vertical axis; M_k is the volumetric interfacial force of phase-k; and F_w is the wall shear force per unit volume, which is defined by:

$$F_w = \frac{1}{2D_H} f\rho_L u_L |u_L|. \quad [3]$$

The interfacial forces being considered in this analysis are defined as:

$$F_d = \frac{1/4\pi D_b^2}{1/6\pi D_b^3} C_d\rho_L(u_G - u_L)|u_G - u_L| = \frac{3}{4} C_d \frac{\rho_L}{D_b}(u_G - u_L)|u_G - u_L|, \quad [4]$$

$$M_L = -M_G = \alpha[F_d + F_{vm}], \quad [5]$$

$$F_{vm} = \rho_L C_{vm} a_{vm}, \quad [6]$$

where D_H is the hydraulic diameter of the flow channel; f is the friction factor; F_d and F_{vm} are the interfacial drag and virtual mass force per unit bubble volume, respectively; D_b is the bubble diameter; C_d is the interfacial drag coefficient; C_{vm} is the virtual volume coefficient; a_{vm} is the steady-state virtual mass acceleration in the axial direction and λ is an arbitrary parameter to be determined experimentally. The most general form of the one-dimensional virtual mass spatial acceleration term is given by (Drew *et al.* 1979)

$$a_{vm} = u_G \frac{d[u_G - u_L]}{dz} + (u_G - u_L)\left\{(\lambda - 2)\frac{du_G}{dz} + (1-\lambda)\frac{du_L}{dz}\right\}. \quad [7]$$

Equations [1] and [2] can be rewritten as,

$$-\frac{dp}{dz} = \rho_L u_L \frac{du_L}{dz} + \rho_L g\cos\phi - \frac{M_L}{(1-\alpha)} + \frac{F_w}{(1-\alpha)}, \quad [8]$$

$$-\frac{dp}{dz} = \rho_G u_G \frac{du_G}{dz} + \rho_G g\cos\phi - \frac{M_G}{\alpha}. \quad [9]$$

Subtracting [9] from [8], to eliminate the pressure gradient,

$$\rho_G u_G \frac{du_G}{dz} = \rho_L u_L \frac{du_L}{dz} + (\rho_L - \rho_G) g\cos\phi - \frac{M_L}{(1-\alpha)} + \frac{M_G}{\alpha} + \frac{F_w}{(1-\alpha)}, \quad [10]$$

or using [5],

$$\frac{du_G}{dz} = \frac{1}{\rho_G u_G}\left\{\rho_L u_L \frac{du_L}{dz} + (\rho_L - \rho_G) g\cos\phi - \frac{(F_d + F_{vm})}{(1-\alpha)} + \frac{F_w}{(1-\alpha)}\right\}. \quad [11]$$

For the cases of interest here, the acceleration of individual bubbles, the void fraction is quite small and thus, [11] can be approximated by,

$$\frac{du_G}{dz} = \frac{1}{\rho_G u_G}\left\{\rho_L u_L \frac{du_L}{dz} + (\rho_L - \rho_G)\, g \cos\phi - F_d - F_{vm} + F_w\right\}, \qquad [12]$$

where we have assumed,

$$\alpha \ll 1. \qquad [13]$$

Equations [11], [3] and [4]–[7] comprise the set of equations which must be integrated to determine the axial velocity of the bubbles, $u_G(z)$.

Before numerical integration can be accomplished, one must have an expression for the spatial acceleration of the liquid, du_L/dz, in [12].

For a conical-shaped nozzle with a linear convergence angle, the radius $R(z)$ is given by,

$$R(z) = R_1 - \frac{z}{H}(R_1 - R_2), \qquad [14]$$

where $R_2 < R_1$ and H is the length of the nozzle (or diffuser).

For the case of interest here, we can neglect the effect of the bubbles, and the liquid continuity equation becomes,

$$u_L(z) = Q/[\pi R^2(z)], \qquad [15]$$

where Q is the volumetric flow rate of the liquid phase. Thus, [15] and [14] yield,

$$\frac{du_L}{dz} = -\frac{2Q}{\pi R^3(z)}\frac{dR}{dz} = \frac{2Q}{\pi R^3(z)}\frac{(R_1 - R_2)}{H}. \qquad [16]$$

Similarly, for a conically-shaped diffuser of linear divergence angle.

$$R(z) = R_1 + \frac{z}{H}(R_2 - R_1), \qquad [17]$$

where $R_2 > R_1$. The corresponding expression for the spatial acceleration of the liquid phase is,

$$\frac{du_L}{dz} = -\frac{2Q}{\pi R^3(z)}\frac{dR}{dz} = -\frac{2Q}{\pi R^3(z)}\frac{(R_2 - R_1)}{H}. \qquad [18]$$

Diffuser/nozzle geometries typical of those analyzed are illustrated in figure 1.

These equations were programmed and numerically integrated, using stiff option of the GEAR algorithm (Gear 1971). For these evaluations, a typical bubble diameter of 0.15 cm was used. For wall shear, a Moody friction factor value of 0.02 was used (i.e. $f = 0.02$); while for interfacial shear, a standard bubble drag coefficient (C_d) was used (Elliot & Weinberg 1968). This latter model is given, for $0.1 < Re \leq 2 \times 10^4$,

$$C_d = 26.33765\, \mathrm{Re}^{-0.8893 + 0.03417 \ln \mathrm{Re} + 0.001443(\ln \mathrm{Re})^2} \qquad [19]$$

where the bubble Reynolds number is defined as,

$$\mathrm{Re} = \frac{\rho_L D_b |u_G - u_L|}{\mu_L}.$$

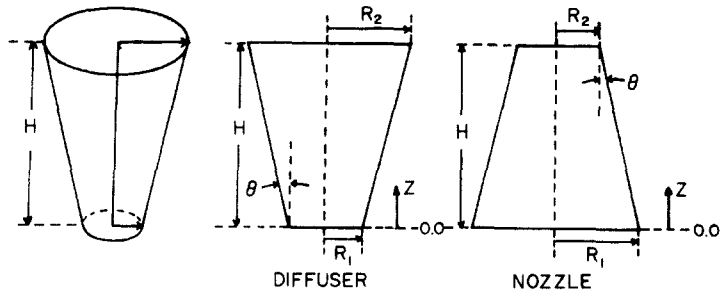

R_1 = INLET RADIUS
R_2 = OUTLET RADIUS
H = AXIAL LENGTH OF DIFFUSER/NOZZLE

FOR A DIFFUSER, $R_1 < R_2$
FOR A NOZZEL, $R_1 > R_2$

DIFFUSER GEOMETRY	NOZZLE GEOMETRY
R_1 = 1.905 CM	R_1 = 5.08 CM
R_2 = 3.175 CM	R_2 = 1.905 CM
H = 19.3675 CM	H = 14.327 CM
θ = 3.75°	θ = 12.5 CM

Figure 1. Diffuser/nozzle geometries.

For the numerical evaluations, the virtual mass model normally used a virtual volume coefficient (C_{vm}) for a perfect sphere, $C_{vm} = 1/2$, although this was varied parametrically. Various models for the acceleration term (a_{vm}) were also used. In particular, several values for the parameter λ in the most general model (Drew *et al.* 1979) were chosen, and the Wallis (1969) model was evaluated. This latter model is a degenerant case of [7], and assumes a spatial acceleration of the form,

$$a_{vm} = u_G \frac{d[u_G - u_L]}{dz}. \qquad [20]$$

Figure 2 shows the results of a hypothetical nozzle experiment for vertical co-current upflow ($\cos\phi = 1$). It can be seen that one cannot easily discriminate between the various a_{vm} models. That is, for the general a_{vm} case, with $\lambda = 1$ and $\lambda = 2$, and the Wallis model, very little difference in $u_G(z)$ was evident. Moreover, even when the virtual mass force was set to zero ($C_{vm} = 0$), the answer was approximately unchanged; although, in this and subsequent cases, the numerics were much less stable and thus integration required a much longer computer run time (about 40 times longer).

Figure 3 shows similar results for a diffuser operated in co-current upflow. Figure 4 shows the results for co-current flow through a horizontal ($\cos\phi = 0$) nozzle. Some differences can be noted between the various virtual mass force acceleration models; however, these differences are again quite small.

Figure 5 shows the results of analyzing co-current downflow ($\cos\phi = 1$) in a nozzle. It is interesting to note that, unlike the previous cases, the buoyancy term causes the vapor velocity to initially be less than the liquid velocity. Since the vapor phase (bubble) has less inertia than the liquid phase, it will accelerate more and, as expected, the vapor velocity will become greater than the liquid velocity. There is a systematic difference noted between the case with no virtual mass ($C_{vm} = 0$) and the other cases; however, this difference is not large.

The final situation investigated was a counter-current vertical ($\cos\phi = 1$) diffuser, in which

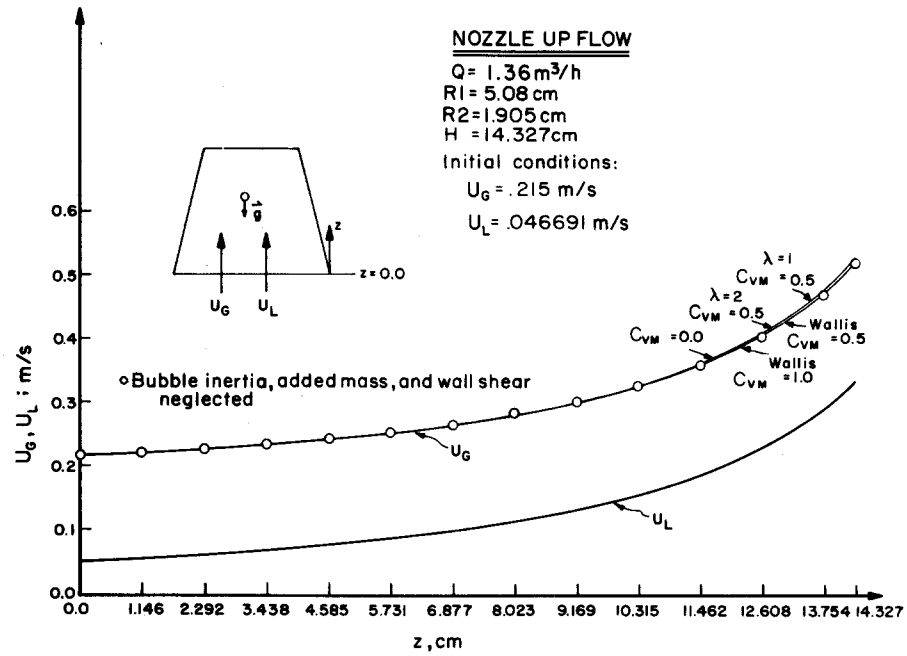

Figure 2. Nozzle upflow.

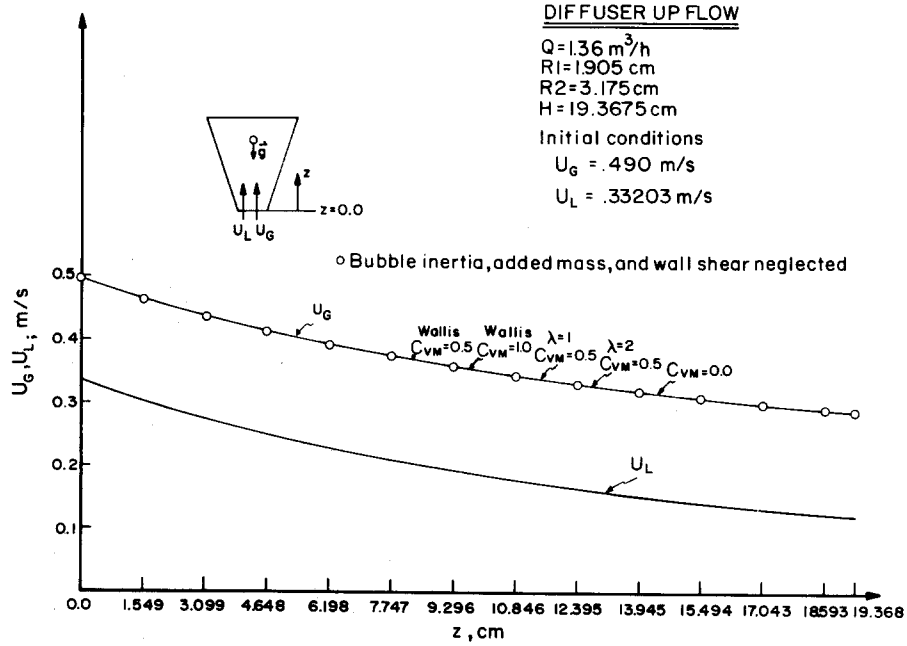

Figure 3. Diffuser upflow.

the liquid is flowing down and the vapor is flowing upwards. In principle, this arrangement allows one to "freeze" the bubble in space. As can be seen in figure 6, the effect of virtual mass is again quite small; however, for the case in which we had no virtual mass force ($C_{vm} = 0$), not only was it more costly to run the problem, but we could not even run the complete problem using GEAR. Thus, even though the virtual mass force may be small, it can be quite important to the numerical evaluation algorithm.

SIMPLIFIED ANALYSIS

The small differences in u_G calculated from the various virtual mass acceleration (a_{vm}) models indicate that the virtual mass effect is insignificant for the flow conditions in question

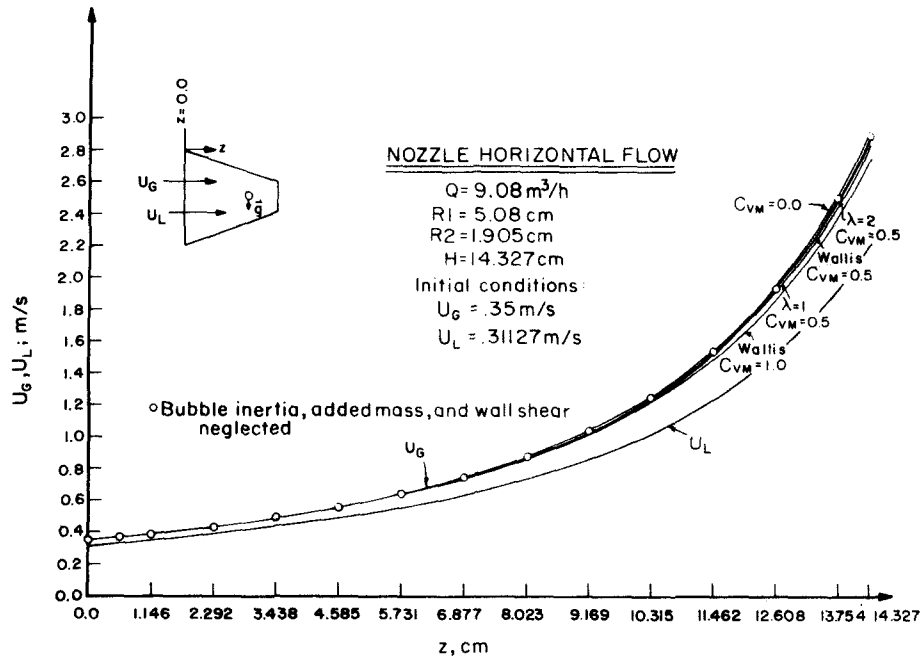

Figure 4. Nozzle horizontal flow.

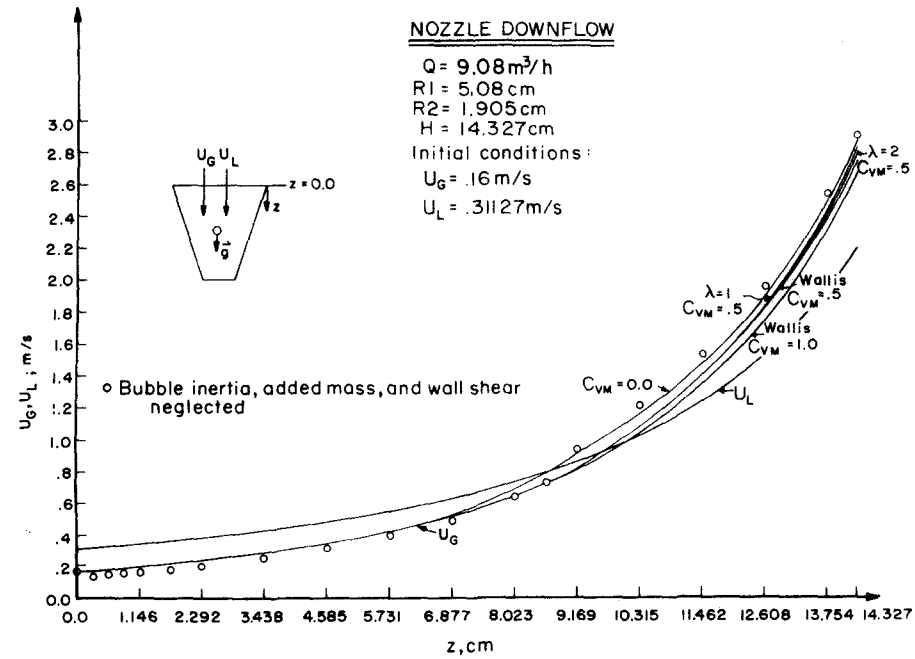

Figure 5. Nozzle downflow.

(i.e. diffuser/nozzle flows). In order to better appraise the importance of vapor phase inertial effects, a simplified analysis of a diffuser/nozzle flow was done ignoring virtual mass, wall shear and terms in the vapor phase momentum equation involving ρ_G (i.e. bubble inertia and density head). That is, we assume,

$$\rho_L \gg \rho_G . \qquad [21]$$

The resultant momentum equation, [12], thus reduces to

$$\rho_L u_L \frac{du_L}{dz} + \rho_L g \cos\phi - F_d = 0 . \qquad [22]$$

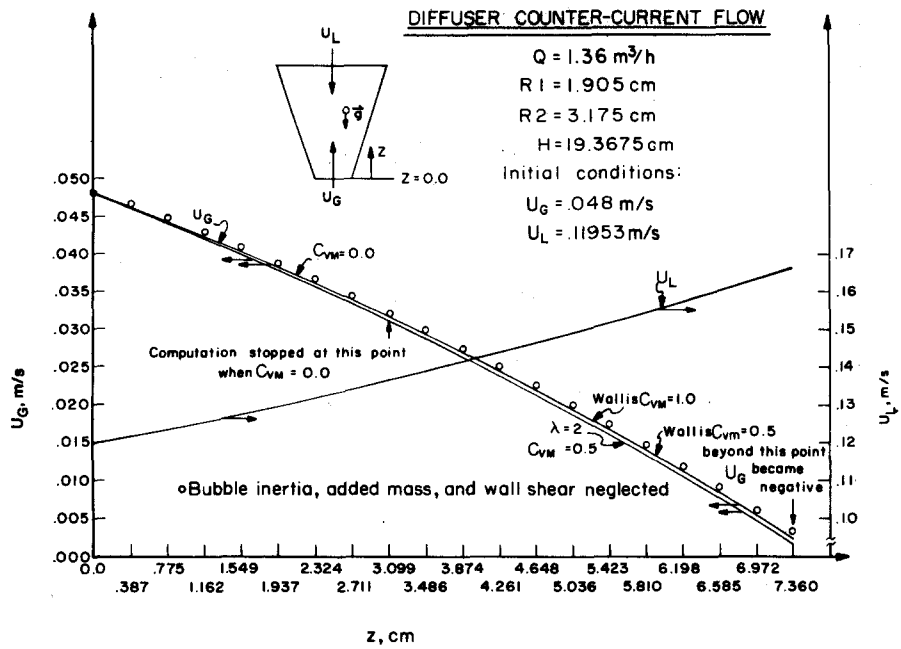

Figure 6. Diffuser counter-current flow.

Using [4], [22] becomes,

$$u_L \frac{du_L}{dz} = -g \cos \phi + \frac{3}{4} C_d \frac{(u_G - u_L)}{D_b} |u_G - u_L| . \qquad [23]$$

In [23], we are essentially balancing the pressure gradient with the buoyancy force and interfacial drag. Rewriting [23] in the form,

$$(u_G - u_L)|u_G - u_L| = \frac{4}{3} \frac{D_b}{C_d} \left\{ u_L \frac{du_L}{dz} + g \cos \phi \right\}, \qquad [24]$$

and defining a new quantity, Φ, where

$$\Phi = \frac{4}{3} \frac{D_b}{C_d} \left\{ u_L \frac{du_L}{dz} + g \cos \phi \right\}. \qquad [25]$$

Equation [24] becomes,

$$(u_G - u_L)|u_G - u_L| = \Phi , \qquad [26]$$

or

$$(u_L - u_G)|u_G - u_L| = -\Phi . \qquad [27]$$

If $u_G > u_L$, [26] yields,

$$u_G = u_L + (|\Phi|)^{1/2} . \qquad [28]$$

If $u_L > u_G$, [27] yields,

$$u_G = u_L - (|\Phi|)^{1/2} . \qquad [29]$$

Equations [28] and [29] give simple, exact, analytical results. When the bubble velocity, $u_G(z)$, is determined from [28] or [29], in which the appropriate expression for nozzle flow, [16], or diffuser flow, [18], is used, the results closely approximate those obtained in the previous, more exact, analysis.

Figures 2 and 3 show the calculated bubble velocity in co-current nozzle upflow and diffuser upflow, respectively. In both cases, the simplified model is just as good in evaluating the bubble velocity as the more involved models. We can thus conclude that pressure gradient, buoyancy, and drag are the dominant forces on a single bubble in nozzle and diffuser flows.

When buoyancy is absent, as in the case shown in figure 4 for co-current flow through a horizontal nozzle, the force balance between the pressure gradient and drag is adequate to describe the motion of a single bubble accelerating through a horizontal nozzle. Indeed, the bubble velocities calculated from the simplified analysis are almost identical to those calculated numerically.

The simplified analysis is compared with the virtual mass acceleration models in figure 5 for co-current downflow in a nozzle. The bubble velocity obtained from the simplified model is now seen to deviate somewhat more from the other models, although the general trend in relative velocity, $u_G - u_L$, is the same as before.

The last case studied was for counter-current flow in a vertical diffuser. As shown in figure 6, in the simplified case the bubble is rising somewhat faster than the bubble having inertial effects. The reason is quite obvious; in the more realistic models (with bubble inertia and virtual mass), the bubble is being slowed down by its own inertia and the added inertia due to virtual mass.

We have found that simplified exact analytical models, which do not involve virtual mass effects, can accurately calculate bubble trajectories. These models confirm the previous numerical results, which indicated that, for the cases considered here, virtual mass effects have little effect on the answer; although they have a pronounced effect on numerical stability and efficiency.

NUMERICAL STABILITY CONSIDERATIONS (STEADY STATE)

In order to understand this paradox, it is convenient to consider a first order, ordinary differential equation given by,

$$\frac{dy}{dz} = f(y, z) \qquad [30a]$$

where

$$y(0) = y_0 . \qquad [30b]$$

If the initial condition is perturbed slightly by an amount δ, we obtain the perturbed differential equation,

$$\frac{du}{dz} = \mu u \qquad [31a]$$

where

$$u(0) = \delta$$

$u = \Delta y$, and for the most general case of a system of differential equations, the μ are the complex eigenvalues of the Jacobian matrix, $(\partial f(y, z)/\partial y)$. Using forward differencing, [31a] becomes,

$$u_{n+1} = u_n + \Delta z \mu u_n \qquad [32a]$$

where

$$u_0 = \delta \qquad [32b]$$

The solution to [32a] and [32b] is given by (Sokolnikoff & Redheffer 1958),

$$u_n = (1 + \Delta z\mu)^n \delta . \qquad [33]$$

The criterion for absolute stability is that the solution function of the perturbation, u_n, will be no larger than $|\delta|$. For this case, [33] implies absolute stability within a unit circle, centered at $(-1, 0)$, in the complex $\Delta z\mu$ plane. That is, where

$$|1 + \Delta z\mu| < 1. \qquad [34]$$

It is significant to note that the real part of μ must be negative for this criterion to be satisfied.

The criterion of absolute stability is too restrictive for many practical purposes. For instance, if the function $y(z)$ increases with z, then one should be able to tolerate a larger perturbation, $u(z)$, in the total solution, $y(z) + u(z)$. Gear (1971) has proposed various other stability criterion. In our case, it is his criterion for an "accurate" numerical solution which imposes the observed restrictions on the spatial step size, Δz.

The stiff option of the Gear algorithm (Gear 1971), which we used in the study, automatically adjusts the step size to achieve an "accurate" solution. If, as shown schematically in figure 7, the system's eigenvalue (μ) is such that the product $\Delta z\mu$ is at point A, then the Gear code would automatically reduce the step size (Δz) to bring the $\Delta z\mu$ product within region R_2 (e.g. to point B). Naturally the smaller the step size, the longer the run time to complete a given problem.

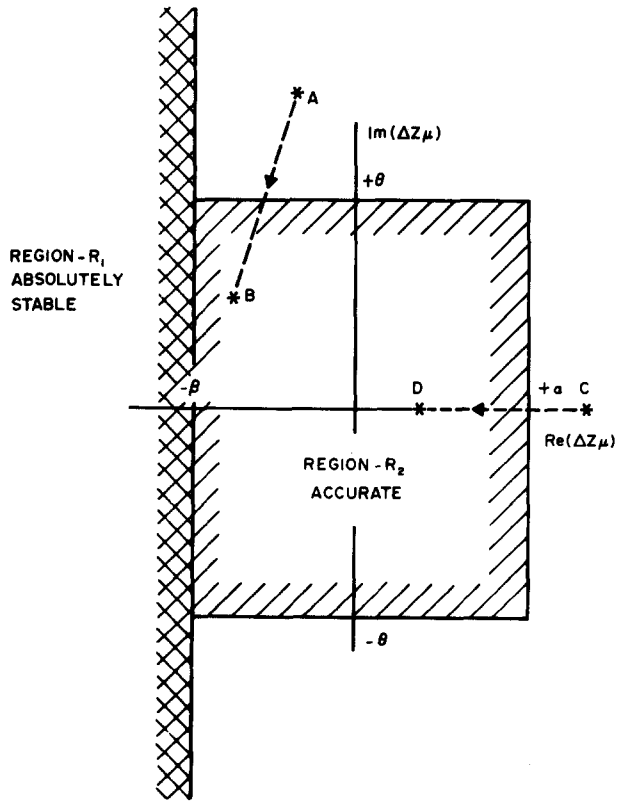

Figure 7. GEAR code stability map.

In our specific case, the eigenvalue (μ) is given by

$$\mu \triangleq \frac{\partial f}{\partial u_G} = \frac{\dfrac{\partial F_w}{\partial u_G} - \dfrac{3}{2}C_d\dfrac{\rho_L}{D_b}|u_G - u_L| - \dfrac{3\rho_L}{4D_b}(u_G - u_L)|u_G - u_L|\dfrac{\partial C_d}{\partial u_G} + \rho_L C_{vm}\lambda\dfrac{du_L}{dz}}{\rho_G u_G + \rho_L C_{vm}\{u_G + (\lambda - 2)(u_G - u_L)\}}$$

$$- \frac{\left[\rho_L u_L \dfrac{du_L}{dz} + (\rho_L - \rho_G)\, g\cos\phi + F_w - \dfrac{3}{4}C_d\dfrac{\rho_L}{D_b}(u_G - u_L)|u_G - u_L| + \rho_L C_{vm}\left\{\lambda u_G\dfrac{du_L}{dz} + (1-\lambda)u_L\dfrac{du_L}{dz}\right\}\right][\rho_G + \rho_L C_{vm}(\lambda - 1)]}{[\rho_G u_G + \rho_L C_{vm}\{u_G + (\lambda - 2)(u_G - u_L)\}]^2} \quad [35]$$

It can be noted that μ is real and positive, and when we have no virtual mass force ($C_{vm} = 0$), it has a large magnitude. This can be seen schematically in figure 7, where for a given Δz, point C is a typical case with no virtual mass ($C_{vm} = 0$); while the point D includes virtual mass. Thus, we find that the stability and efficiency of the numerical solution is determined by the mathematical nature of the eigenvalue (μ). In this case, μ has a large positive real part, thus we must have a small spatial step (Δz) in order to insure an accurate solution.

NUMERICAL STABILITY CONSIDERATIONS (TRANSIENTS)

Let us now investiagte the more general case of the effect of virtual mass on the eigenvalues of a transient two-phase system. To simplify the analysis, the equations for incompressible air/water flow in a constant area duct are used, since the basic classification of the system is not affected by these simplifying assumptions. The one -dimensional phasic continuity equations are,

$$\frac{\partial \alpha}{\partial t} + \frac{\partial[\alpha u_G]}{\partial z} = 0\,, \quad [36a]$$

$$\frac{\partial(1-\alpha)}{\partial t} + \frac{\partial[(1-\alpha)u_L]}{\partial z} = 0\,. \quad [36b]$$

The corresponding one-dimensional phasic momentum equations are,

$$\alpha\rho_G\left[\frac{\partial u_G}{\partial t} + u_G\frac{\partial u_G}{\partial z}\right] = -\alpha\frac{\partial p}{\partial z} - \alpha\rho_G g\cos\phi + M_G \quad [37]$$

$$(1-\alpha)\rho_L\left[\frac{\partial u_L}{\partial t} + u_L\frac{\partial u_L}{\partial z}\right] = -(1-\alpha)\frac{\partial p}{\partial z} - (1-\alpha)\rho_L g\cos\phi + M_L - F_w \quad [38]$$

where

$$M_G = -\alpha[F_d + F_{vm}]$$

$$M_L = \alpha[F_d + hF_{vm}] \quad [39b]$$

$$F_{vm} = \rho_L C_{vm}\left\{\frac{\partial u_G}{\partial t} - \frac{\partial u_L}{\partial t} + u_G\frac{\partial u_G}{\partial z} - u_G\frac{\partial u_L}{\partial z} + w\left[(\lambda-2)(u_G - u_L)\frac{\partial u_G}{\partial z} + (1-\lambda)(u_G - u_L)\frac{\partial u_L}{\partial z}\right]\right\}. \quad [39c]$$

We note that if we let $h = 0$ and $w = 0$, we have the model proposed by Hinze (Hinze 1961), in which the virtual mass force (F_{vm}) appears only in the vapor phase momentum equation, and

the last term in [39c] does not appear. If we let $h = 1$ but $w = 0$, we obtain the model proposed by Wallis (1969), and if we let $h = 1$, $w = 1$ and λ be arbitrary, we get the most general case, in which the virtual mass force is objective (Drew *et al.* 1979).

It is convenient to eliminate the pressure gradient $(\partial p/\partial z)$ between [37] and [38]. If we multiply [38] by $\alpha/(1-\alpha)$ and subtract it from [37], we obtain,

$$\alpha\rho_G\left[\frac{\partial u_G}{\partial t}+u_G\frac{\partial u_G}{\partial z}\right]-\alpha\rho_L\left[\frac{\partial u_L}{\partial t}+u_L\frac{\partial u_L}{\partial z}\right]$$
$$=\alpha(\rho_L-\rho_G)\,g\cos\phi-\frac{\alpha}{(1-\alpha)}F_d+\frac{\alpha}{(1-\alpha)}F_w-\alpha\left(1+\frac{\alpha h}{1-\alpha}\right)F_{vm}. \qquad [40]$$

Equations [36] and [40] can be written in matrix form as

$$\mathbf{A}\frac{\partial u}{\partial t}+\boldsymbol{B}\frac{\partial u}{\partial z}=c, \qquad [41]$$

where

$$u=[\alpha, u_G, u_L]^T, \qquad [42a]$$

$$\mathbf{A}=\begin{bmatrix}1 & 0 & 0\\ -1 & 0 & 0\\ 0 & a_{32} & a_{33}\end{bmatrix} \qquad [42b]$$

with

$$a_{32}=\alpha\rho_G+\alpha\left(1+\frac{\alpha h}{1+\alpha}\right)C_{vm}\rho_L \qquad a_{33}=-\rho_L\alpha^2\left(1+\frac{\alpha h}{1-\alpha}\right)C_{vm}\rho_L$$

and

$$\mathbf{B}=\begin{bmatrix}u_G & \alpha & 0\\ -u_L & 0 & (1-\alpha)\\ 0 & b_{32} & b_{33}\end{bmatrix} \qquad [42c]$$

with

$$b_{32}=u_G\left[\alpha\rho_G+\alpha\left(1+\frac{\alpha h}{1-\alpha}\right)\rho_L C_{vm}\right]+(u_G-u_L)\left[w\alpha\left(1+\frac{\alpha h}{1-\alpha}\right)(\lambda-2)\rho_L C_{vm}\right]$$

$$b_{33}=-\left[\alpha\rho_L u_L+\alpha\left(1+\frac{\alpha h}{1-\alpha}\right)\rho_L C_{vm}u_G\right]+(u_G-u_L)\left[w\alpha\left(1+\frac{\alpha h}{1+\alpha}\right)\rho_L C_{vm}(1-\lambda)\right].$$

The characteristics of [41] are given by,

$$\frac{dz}{dt}=v_{i(i=1,2,3)} \qquad [43]$$

where v_i are the eigenvalues of the transient system and are given by (Garabedian 1964)

$$\det[Av-B]=0. \qquad [44]$$

Combining [42b], [42c] and [44], and expanding out the determinant, we obtain an algebraic equation of the form,

$$V^2\left\{a\left(\frac{Y}{V}\right)^2+b\left(\frac{Y}{V}\right)+c\right\}=0 \qquad [45]$$

where

$$Y \triangleq v - u_G \tag{46a}$$

$$V \triangleq u_G - u_L \tag{46b}$$

and

$$a = (1-\alpha)\left\{\alpha\rho_G + \alpha\left[1+\frac{\alpha h}{(1-\alpha)}\right]\rho_L C_{vm}\right\} + \alpha^2\rho_L + \alpha^2\left[1+\frac{\alpha h}{(1-\alpha)}\right]\rho_L C_{vm} \tag{47a}$$

$$b = w\alpha(1-\alpha)\left[1+\frac{\alpha h}{(1-\alpha)}\right](2-\lambda)\rho_L C_{vm} + 2\alpha^2\rho_L + \alpha^2\left[1+\frac{\alpha h}{(1-\alpha)}\right]\rho_L C_{vm}[1+w(1-\lambda)] \tag{47b}$$

$$c = \alpha^2\rho_L + w\alpha^2\left[1+\frac{\alpha h}{(1-\alpha)}\right]\rho_L C_{vm}(1-\lambda)\,. \tag{47c}$$

The roots of the quadratic equation, [45], are, given by

$$v = \frac{[-b \pm \sqrt{(b^2-4ac)}]}{2a}(u_G - u_L) + u_G\,. \tag{48}$$

Based on physical reasoning, we would expect the system of partial differential equations to be hyperbolic (Garabedian 1964). For the system to be hyperbolic, we must have two† real, distinct roots (v_1 and v_2). The most general case is that of slip flow, where, $V \neq 0$. Thus, in order to have two real, distinct roots, [48] implies we must have,

$$b^2 - 4ac > 0\,. \tag{49}$$

For Hinze's model ($h = 0$, $w = 0$), [49] implies,

$$C_{vm} > \frac{4(1-\alpha)}{\alpha} \tag{50}$$

and [47b] yields

$$b = \alpha^2\rho_L[2 + C_{vm}]\,. \tag{51}$$

For Wallis' model ($h = 1$, $w = 0$), [49] implies,

$$C_{cm} > \frac{4(1-\alpha)^2}{\alpha} \tag{52}$$

and [47b] yields,

$$b = \alpha^2\rho_L[2 + C_{vm}/(1-\alpha)]\,. \tag{53}$$

For the most general virtual mass model ($h = 1$, $w = 1$ and λ arbitrary), [49] implies

$$\lim_{\alpha\to 0} C_{vm} > 0 \tag{54}$$

†The third root is $dt/dz = 0$, and results from the assumption of incompressibility.

(for $\lambda < 2$) and [47b] yields

$$b = \alpha^2 \rho_L \left\{ 2 + \frac{C_{vm}}{\alpha(1-\alpha)} (2-\lambda) \right\}. \quad [55]$$

Finally, for the case in which we have no virtual mass model ($C_{vm} = 0$), [47b] yields

$$b = 2\alpha^2 \rho_L \quad [56]$$

and [49] shows that we will always have complex conjugate roots; i.e.

$$b^2 - 4ac = -4\alpha^3 \rho_L \rho_G (1-\alpha). \quad [57]$$

It is interesting to note that for reasonable values of the virtual volume coefficient ($C_{vm} = 1/2$), and conditions typical of bubbly flow ($\alpha \leq 0.3$), all cases investigated have complex conjugate eigenvalues. It is significant, however, that for the most general virtual mass acceleration model, [55] indicates that the real part ($b/2a$) of the eigenvalue is the largest (and thus most negative), and the imaginary part is the smallest. In contrast, for the case involving no virtual mass term, [56] indicates that the real part ($b/2a$) is the smallest (and thus the least negative), and the imaginary part is the largest of all the cases investigated. Previous investigators (Ramshaw & Trapp 1978) have shown that complex characteristics lead to numerical stability problems, thus, it is clear why the inclusion of a virtual mass model improves the numerical stability and efficiency of both transient and steady two-phase flow problems.

SUMMARY AND CONCLUSIONS

This paper has focused on the effect virtual mass models have on the numerical stability and efficiency of accelerating two-phase flows. It has been found, in actual calculations of nozzle/diffuser geometries, that the inclusion of appropriate virtual mass models decreases the run time by more than an order of magnitude. An investigation of the eigenvalues of the mathematical system, and the stability of typical numerical algorithms, such as those due to Gear (1971), have shown that appropriate virtual mass models improve stability and efficiency by reducing the modulus of the eigenvalues.

While it is true that the use of other algorithms, which introduce so-called "numerical viscosity", can also yield corresponding reductions in run time, virtual mass effects cannot, in general, be neglected. In the cases investigated in this study, nozzle/diffuser flows, the effect of the virtual mass force on the solution was small, and thus techniques employing "numerical viscosity" should yield good results. For other cases of practical concern, such as critical flow, which involve large accelerations, one would expect virtual mass effects to be quite important, and thus any model which neglects these effects could give large errors. Thus, the inclusion of virtual mass effects into the analysis of steady or transient two-phase flow appears to be a physically realistic way to improve numerical stability and efficiency, and to achieve accurate results in many cases of practical concern.

Acknowledgements—The support given this work by the USNRC under Contract NRC-04-76-301, is gratefully acknowledged.

REFERENCES

AMSDEN, A. A. & HARLOW, F. H. 1978 K-TIF: A two-fluid computer program downcomer flow dynamics. LA-6994, NRC-4.

BOURÉ, J. 1975 On a unified presentation of the non-equilibrium two-phase flow models. ASME Symp. Volume, *Non-Equilibrium Two-Phase Flows.*

DREW, D., CHENG, L. & LAHEY, R. T. Jr. 1979 The analysis of virtual mass effects in two-phase flow. *Int. J. Multiphase Flow* **5**, 233–242.

ELLIOT, D. G. & WEINBERG E. 1968 Acceleration of liquids in two-phase nozzles. JPL Tech. Rep. 32–987.

GARABEDIAN, P. R. 1964 *Partial Differential Equations*. Wiley, New York.

GEAR, C. W. 1971 *Numerical Initial Value Problems in Ordinary Differential Equations*. Prentice-Hall, Englewood Cliffs, New Jersey.

HINZE, J. O. 1961 Momentum and mechanical energy balance equations for a flowing homogeneous suspension with slip between the two phases. *Appl. Sci. Res.* Section-A, Vol. II.

ISHII, M. 1975 *Thermo-Fluid Dynamic Theory of Two-Phase Flow*. Eyrolles, Paris.

RAMSHAW, J. D. & TRAPP, J. A. 1978 Characteristics, stability, and short-wavelength phenomena in two-phase flow equations systems. *ANS J. Nucl. Science Engng* **66**, 93–102.

SOKOLNIKOFF, I. S. & REDHEFFER, R. M. 1958 *Mathematics of Physics and Modern Engineering*. McGraw-Hill, New York.

WALLIS, G. B. 1969 *One-Dimensional Two-Phase Flow*. McGraw-Hill, New York.

WALLIS, G. B., RICHTER, H. J. & KUO, J. T. 1976 The separated flow model of two-phase flows. EPRI-NP-275.